Energy & Environmental Science

ROYAL SOCIETY OF CHEMISTRY

REVIEW

View Article Online
View Journal | View Issue

Published on 23 September 2014. Downloaded by California Institute of Technology on 20/03/2015 15:15:34.

Cite this: *Energy Environ. Sci.*, 2015, **8**, 423

Measuring thermoelectric transport properties of materials

Kasper A. Borup,[a] Johannes de Boor,[b] Heng Wang,[c] Fivos Drymiotis,[c] Franck Gascoin,[d] Xun Shi,[e] Lidong Chen,[e] Mikhail I. Fedorov,[fg] Eckhard Müller,[bh] Bo B. Iversen[a] and G. Jeffrey Snyder*[cg]

Received 28th April 2014
Accepted 23rd September 2014

DOI: 10.1039/c4ee01320d

www.rsc.org/ees

In this review we discuss considerations regarding the common techniques used for measuring thermoelectric transport properties necessary for calculating the thermoelectric figure of merit, *zT*. Advice for improving the data quality in Seebeck coefficient, electrical resistivity, and thermal conductivity (from flash diffusivity and heat capacity) measurements are given together with methods for identifying possible erroneous data. Measurement of the Hall coefficient and calculation of the charge carrier concentration and mobility is also included due to its importance for understanding materials. It is not intended to be a complete record or comparison of all the different techniques employed in thermoelectrics. Rather, by providing an overview of common techniques and their inherent difficulties it is an aid to new researchers or students in the field. The focus is mainly on high temperature measurements but low temperature techniques are also briefly discussed.

Measurement guide for authors and reviewers

Measurements should always be repeatable on the same sample, and on new samples produced in the manner described. Thermoelectric effects are steady-state effects so any time dependence or hysteresis is indication that phenomena outside thermoelectric effects are at play. Materials with chemical oxidants/reductants incorporated are likely to contain unstable internal voltages not due to thermoelectric effects. Unconventional samples or measurement methods deserve reexamination of assumptions.

Accuracy

True accuracy is not represented by a single heating curve from one sample, even with error bars representing instrument precision. Showing heating and cooling data and multiple samples gives a better indication of measurement variability for a typical type of sample. Anisotropy, cracks and inhomogeneities can lead to large variation in measurements. One unusual data point or sample outside the trend, particularly at temperatures just prior to decomposition, usually indicates a problem in sample or measurement.

Unusual results

Typical thermoelectric materials behave like heavily doped semiconductors with thermopower (absolute value of Seebeck coefficient) of less than 300 $\mu V K^{-1}$, resistivity of 0.1–10 mΩ cm, and are optimized when electronic contribution to the thermal conductivity is about 1/2 the total thermal conductivity. Extraordinary results should be checked by extra means. Unusual results can be caused by bad contacts, thermocouples that have broken, chemically reacted, or simply drifted out of calibration.

Exceptional results

Reported values of $zT > 1$ or in unexpected materials receive extra attention from reviewers who may ask for additional confirmation. Convincing measurements may need to be performed on the same sample along the same direction and be repeatable with other samples and measurement methods. There is no official record keeping for claimed or verified *zT* values. Several papers, patents and press releases have claimed extraordinarily high *zT* but most have been forgotten over time and likely resulted from incorrect measurements.

[a] Center for Materials Crystallography, Department of Chemistry and iNANO, Aarhus University, DK-8000 Aarhus, Denmark
[b] Institute of Materials Research, German Aerospace Center, Linder Höhe, D-51147 Cologne, Germany
[c] Materials Science, California Institute of Technology, Pasadena, California 91125, USA. E-mail: jsnyder@caltech.edu
[d] Laboratoire CRISMAT UMR 6508 CNRS ENSICAEN, 14050 Caen Cedex 04, France
[e] State Key Laboratory of High Performance Ceramics and Superfine Microstructure, Shanghai Institute of Ceramics, Chinese Academy of Sciences, Shanghai 200050, China
[f] Ioffe Physical-Technical Institute, St Petersburg 194021, Russian Federation
[g] ITMO University, Saint Petersburg, Russia
[h] Justus Liebig University Giessen, Institute of Inorganic and Analytical Chemistry, D-35392 Giessen, Germany

This journal is © The Royal Society of Chemistry 2015

Published on 23 September 2014. Downloaded by California Institute of Technology on 20/03/2015 15:15:34.

Introduction

Thermoelectric materials are a group of electronic materials which can interconvert gradients in electrical potential and temperature.[1] Thermoelectrics can be used for both cooling and power generation.[2,3] The first is widely used for cooling delicate optoelectronics, detectors, and small scale refrigeration. The latter has successfully been used for power generation in deep space missions[4] but is now proposed for waste heat recovery, *e.g.* in vehicles,[5] or for wireless remote sensing such as in aircraft.[6,7] While the impact on global energy consumption may not necessarily be large,[8] niche applications abound as materials are improved and novel materials commercialized. Since thermoelectric devices are solid state and contain no moving parts, they find application because they are easily scalable and require little maintenance even though they are inferior in efficiency compared to traditional dynamic heat engine/refrigeration methods.[2,3,5]

The physics of thermoelectrics are governed by three thermodynamic effects, the Seebeck, Peltier, and Thomson effects. These have a common physical origin and are related through the Seebeck coefficient. The Seebeck effect generates an electrical potential gradient when a temperature gradient is applied (used for power generation), while the Peltier effect pumps reversible heat and can thus establish a temperature gradient when a current is passed through the material (used for cooling). Thomson heat is released or absorbed internally in a material if the Seebeck coefficient depends on temperature, balancing for the flowing Peltier heat. All effects are related to heat being transported by the charge carriers. While the effects were discovered in metals, modern thermoelectric materials are heavily doped semiconductors. Both n- and p-type materials are used and both are needed in a device.

The maximum efficiency of a thermoelectric material, whether in cooling or power generation, is depending upon the thermoelectric figure of merit, zT,

$$zT = \frac{S^2}{\rho\kappa}T. \tag{1}$$

S is the Seebeck coefficient, ρ is the electrical resistivity, κ is thermal conductivity, and T is absolute temperature. The device efficiency is given by the Carnot efficiency, $(T_h - T_c)/T_h$, multiplied by a complicated function of the properties and geometry of the materials and device. This function generally increases monotonously with the average of zT of the two materials across the temperature range used.[9,10]

With the continued growing interest in the development of better materials, where even a 20% improvement over state-of-the-art would make significant commercial impact, measurement accuracy is of critical importance. For example, excessively large electrical contacts in resistivity and Hall effect measurements lead to misinterpretation of the transport properties and inaccurate reports of Seebeck enhancement in PbTe-based quantum dot superlatices.[11–13] Conversely, early measurements and estimates of the high temperature thermal conductivity of the lead chalcogenides are some 30% higher than the values obtained today resulting in an underestimation of zT for decades.[14,15] Such discrepancies are to be expected even today as absolute accuracy in thermoelectric measurements is still not possible; even published results on standards should be periodically reevaluated. The Seebeck coefficient is particularly difficult as it is inherently a relative measurement. While instruments with identical geometries often give similar values, estimating the relative accuracy of different geometries is more difficult. In one study, the off-axis 4-point geometry was found to overestimate the Seebeck coefficient relative to the 2-point geometry due to cold finger effects. The overestimation was found to be proportional to the temperature difference between the sample and surroundings, reaching 14% at 900 K.[16,17]

While there are many recent studies and prior reviews on thermoelectric measurements and instrumentation, data treatment, and developing new methods[16–23] this is often highly specialized work and may not be readily accessible or seem overwhelming to new researchers or research groups in the field. We here present a review of the most common techniques used for measuring the transport properties necessary to characterize a bulk thermoelectric material. The main focus is on techniques for characterization at room temperature and above, but some low temperature techniques are also briefly included. Common problems encountered when using each technique are discussed as well as their advantages, disadvantages, and limitations. The effects of various user or instrument errors on the results are discussed to aid the researcher in identifying erroneous data early in the characterization process.

General considerations

In order to direct material development, high precision measurement of zT as well as good estimates of the error is necessary. Due to the lack of appropriate standard reference materials, especially at high temperatures, true measurement accuracy is not known. Propagation of the statistical uncertainties of the individual measurements does not give a good estimate for the accuracy, but instead gives an estimate of the data quality. In a recent round-robin by Hsin Wang *et al.*,[24] the scatter in zT was estimated to be 12% at 300 K when comparing data on the same material measured at several laboratories. This increased to 21% at 475 K; above this temperature higher variation can be expected. The scatter is defined as the maximum spread in data divided by the average.

Before characterization of a bulk sample, its density needs to be evaluated. The theoretical density can be calculated from the unit cell size and contents, and from this the relative density can be calculated. This is usually greater than 98% for dense samples. The measured zT often deviates from that of a dense sample when the relative density is less than 90% and suspect when less than 97%.[25]

Internal standards

Commercial standards with properties close to typical values for thermoelectrics are not available for all measurements. Hence it

 This journal is © The Royal Society of Chemistry 2015

Published on 23 September 2014. Downloaded by California Institute of Technology on 20/03/2015 15:15:34.

is recommended that laboratories develop internal standards. These can be materials the group has some experience working with and that are stable in the desired temperature range and with repeated thermal cycling. Elements with high vapor pressure, easily oxidized materials, or materials which can potentially react with thermocouples or contacts should be avoided. While such laboratory standards do not provide an estimate of apparatus accuracy, they are useful for identifying instrument drift and other errors. For example, thermocouple drift at elevated temperatures can be well in excess of 10 K due to thermocouple ageing or reactivity with samples or environment. This can potentially cause large systematic errors in Seebeck measurements.

Even with apparently trivial measurements, skill and experience can be required to obtain high quality measurements. Hence, when training new researchers or students, having them repeatedly mount and measure an internal standard until consistent and accurate results are obtained ensures proper instrument use. Especially when both good electrical and thermal contact is required at multiple points, inexperience can lead to erroneous measurements. This may not always be obvious from the measurement itself, and hence using a standard is recommended.

Sample homogeneity

There are two different types of inhomogeneity worth distinguishing: multi-phase inhomogeneity and charge carrier concentration (dopant) fluctuations. The first is normally detected by powder X-ray diffraction (PXRD) when large amounts (>2–5%) of impurities are present. Small amounts of impurities or amorphous phases are more easily detected by microscopy (*e.g.* scanning electron microscopy (SEM)).[26,27] The effect of secondary phases is strongly linked to the shape of inclusions. While a few volume percent of dispersed compact impurities normally do not affect the transport properties (especially Seebeck coefficient), insulating or metallic phases or cracks along grain boundaries may significantly influence the electrical and thermal conductivities. The presence of impurities may change the dopant content and hence charge carrier concentration of the main phase. For materials where the charge carrier concentration can be estimated from simple charge counting (*e.g.* using the Zintl principle)[28–32] comparison of stoichiometry (nominal and *e.g.* Electron Microprobe Analysis) with the measured Hall effect charge carrier concentration can be used to check for this. A sample falling outside the general trend calls for further examination.

Post synthesis processing, *e.g.* ball milling, hot pressing, spark plasma sintering (SPS), annealing, *etc.* may develop secondary phases or otherwise change the material, particularly in SPS where large DC currents may drive mobile species.[33–37] Again while scanning PXRD and SEM are powerful tools for investigating purity, they may completely miss dopant variations.[38] Instead, spatially resolved scanning Seebeck coefficient measurements[38–41] (*e.g.* PSM from Panco Gmbh, Germany) can detect these variations and thus provide an important complementary technique for establishing homogeneity and quality control of bulk materials.

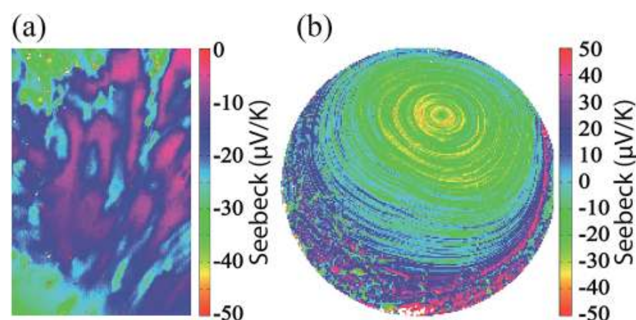

Fig. 1 Scanning Seebeck plots of a $Ba_8Ga_{16}Si_{30}$ raw synthesis product (a) and a Bridgman grown $PtSb_2$ single crystal (b). In (a), the scan is 3.275×4.85 mm^2 with a resolution of 0.025 mm and in (b) 9 mm in diameter with 0.05 mm resolution.

Even materials (both single crystals and polycrystalline materials) believed to melt congruently will in general produce doping inhomogeneity during solidification from the melt.[42] Fig. 1a shows a scanning Seebeck map of melt solidified $Ba_8Ga_{16}Si_{30}$ displaying a solidification microstructure not seen in PXRD or SEM. Such dopant gradients can also be observed and controlled in Bridgman grown single crystals of $PtSb_2$ (Fig. 1b) which clearly demonstrates that single crystals are not necessarily homogeneous.[43]

Powdered, hot pressed, and solid-state annealed samples are typically better to ensure homogeneous charge carrier concentration on the macroscopic and microscopic level.[42–44] Inhomogeneities can potentially cause large errors in zT if all properties are measured on different samples or in some cases along different directions.

Seebeck coefficient

A variation of about 5% in measured Seebeck coefficient can generally be expected at room temperature.[45–47] This will, however, also depend on the method employed.[17] The differences between the methods and possible ways to improve the results are discussed below. The accuracy of Seebeck coefficient measurements is unknown since it can only be measured relatively between two materials. A standard reference material (NIST SRM 3451) is available in the temperature range 10–390 K. At higher temperatures no appropriate standard reference materials are available. Constantan, chromel, and other thermocouple alloys have well determined Seebeck coefficients; however, the values fall outside the range of interest for thermoelectrics.

Measurements and data extraction

The Seebeck coefficient is the ratio of a resulting electric field gradient to an applied temperature gradient. While the Seebeck coefficient is conceptually simple, in reality it can be difficult to measure accurately. A recent review addresses some of the instrument design challenges,[48] while another studies data

Published on 23 September 2014. Downloaded by California Institute of Technology on 20/03/2015 15:15:34.

analysis.[49] In a typical measurement, the temperature is varied around a constant average temperature and the slope of the voltage (V) *vs.* temperature difference (ΔT) curve gives the Seebeck coefficient (the slope method) or just $V/\Delta T$ is measured (single point measurement). Either a specific temperature difference is stabilized before each measurement (steady-state), which takes longer,[16,50,51] or measurements are conducted continuously while the temperature difference is varied slowly (quasi-steady-state).[16,19,52,53] In a recent study,[17] little difference was found between steady-state and quasi-steady-state measurements when good thermal and electrical contact is ensured.

The employed temperature difference should be kept small, but too small will lead to decreased accuracy. Usually 4–20 K (or ±2–±10 K) is appropriate for the full temperature span. When using the quasi-steady-state method, all voltages and temperatures should ideally be measured simultaneously[16,48] or timed using the "delta measurement" technique (individual voltage measurements performed symmetrically in time) or with time stamps to compensate for a linear drift.[19,49]

In the slope method the measured raw data is corrected for constant offset voltages by using the slope of several (ΔT,V) points for extracting the Seebeck coefficient.[16,19,48,49] The offset voltages can reach several hundred microvolts, increasing at elevated temperatures and can be caused by several effects, including differences in thermocouple wires, reactive samples, and the cold finger effect (heat being drawn away from the sample through the thermocouple, causing a temperature drop between the sample and thermocouple tip due to the thermal contact resistance). It is an open circuit voltage and is not usable for continuous power generation since a heat engine cannot output power without a heat flow. The single point method is unable to separate this from the actual Seebeck coefficient. The slope method, in contrary, is designed to extract only the thermoelectric part of the voltage, provided the offset is constant during one measurement. Most commercial systems (including the ZEM series by ULVAC-Rico) use the slope method to extract the Seebeck coefficient from steady-state measurements.

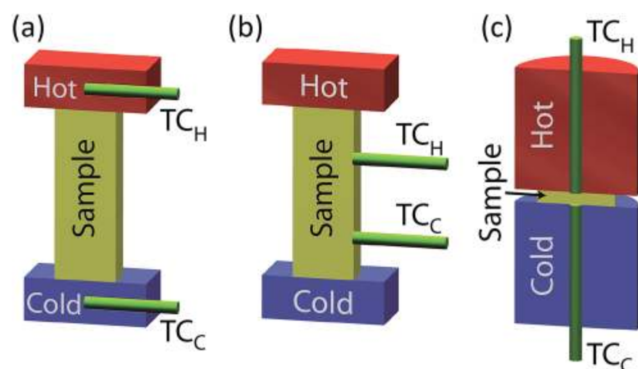

Fig. 2 The three common geometries for Seebeck coefficient measurements in cross sectional view: 2-point (a), off-axis 4-point (b) and uniaxial 4-point (c). The upper and lower heaters are shown in red and blue, the sample in between the two heaters in yellow, and the thin thermocouple rods in green. The thermal gradient can be applied in both directions.

Instrument geometries

The contact arrangement is also of importance. Generally three different geometries exist:[19,48] 2-point (Fig. 2a), off-axis 4-point (Fig. 2b), and uniaxial 4-point (Fig. 2c). It is important to minimize electrical and thermal contact resistances and make sure the temperature and voltage are measured at the same point in space. This is not realized in the 2-point geometry, where thermocouple and voltage leads are generally imbedded in metallic contact pads in the heaters, however, the error may be small when good thermal and electrical contact is made to the sample (*e.g.* by soldering or using pads of high thermal conductivity metals such as tungsten).[17] The 2-point geometry is also often used where other considerations than accuracy are important, such as in scanning systems.[39]

In the off-axis 4-point geometry the thermocouples and voltage leads are pressed against the sides of the sample thus allowing concurrent measurement of Seebeck and resistivity during one measurement run. This method is used in the most popular commercial instruments (*e.g.* by ULVAC-Rico or Linseis). Here the thermocouples are in direct contact with the sample, reducing the distance between the electrical and thermal contacts. Since only low force can be used on the thermocouples to avoid bending (some materials may turn soft at high temperatures), breaking or shifting the sample, the thermal and electrical contact resistance may actually be large. High thermal conductivity alumina sheathed thermocouples extend to outside the heated zone to a chamber near room temperature. They may thus act as cold fingers and create a temperature gradient across the thermocouple tip-sample interface. The thermocouples would then underestimate each temperature and also ΔT, leading to an overestimated thermopower (absolute value of Seebeck coefficient).[17,19] The analysis of the cold finger effect by Martin[17] further implies that the average temperature of the two thermocouples (which is used as the sample temperature) underestimates the true average temperature of the sample. This effect is expected to be a linear function of the temperature difference between the sample and surroundings and will compress the temperature interval of the measured Seebeck coefficient. If the Seebeck coefficient has strong temperature dependence this can affect the accuracy significantly. A large deviation between the temperatures of the gradient heaters in direct contact with the sample and average sample temperature can be an indication that cold finger effects are affecting the measurement accuracy.

In a recent study by Martin[17] the results from the 2-point and off-axis 4-point geometries were compared. The off-axis 4-point geometry was observed to yield thermopower values higher than the 2-point geometry, with the difference being proportional to the temperature difference between the sample and surroundings. With a thorough analysis of the thermal resistances the study concludes that the cold finger effect is responsible for the higher thermopower values and that the 2-point geometry is preferable.

 This journal is © The Royal Society of Chemistry 2015

Published on 23 September 2014. Downloaded by California Institute of Technology on 20/03/2015 15:15:34.

The uniaxial 4-point geometry was developed to remedy these problems. The cold finger effect is reduced by inserting the thermocouples through the heaters, while the thermal contact resistance is kept low by having the thermocouples in direct contact with the sample with independent, constant pressure. The thermocouples may act as both cold and hot fingers in this geometry, depending on the strength of the thermal coupling to the heaters. Due to the heaters, the cold finger effect will be reduced compared to the 4-point off-axis geometry and since the temperature difference between the heater and sample is small, the hot finger effect is also believed to be small. With bad thermal contact in this setup, the thermocouples can both over- and underestimate the temperature and ΔT, depending on whether they act as cold or hot fingers; however, the error is believed to be smaller than for the 4-point off-axis geometry. The thin sample geometry with high cross sectional area leads to a high heat flux compared to the off-axis geometry and may increase the temperature drop across the heater–sample and thermocouple–sample interfaces. If each sample–heater and sample–thermocouple interface is not of approximately equal quality, it can be difficult to keep the average sample temperature constant during a ΔT sweep.

At low temperatures, the Quantum Design, Physical Property Measurement System (PPMS) has been extensively used. In the Thermal Transport Option (TTO), four copper leads are attached to a bar sample with conductive adhesive and a heater, two resistance thermometers and a heat sink are mechanically attached to these (corresponding to the off-axis 4-point geometry but without the thermocouples in direct contact with the sample). Hence, the temperature and voltage are measured far from each other and the cold-finger effect may be large. This geometry is further discussed in the section on thermal conductivity.

Thermal and electrical contact

If possible, points should be measured for both increasing and decreasing ΔT and the data checked for hysteresis, such as in Fig. 3b. Hysteresis can be an indication of poor thermal contact between sample and thermocouples or heaters. In Fig. 3a measurements with good and bad thermal contact are shown. Thermal voltages resulting from temperature changes in the wiring can also lead to hysteresis. The later can be checked by heating local areas around the sample stage with a heat gun or soldering tip. Using higher pressure on the thermocouples or inserting a thin piece of graphite foil may help improving thermal contact. When combining resistivity and Seebeck measurements, the graphite may significantly increase the contact size and hence affect the resistivity measurement and should be used with care.

Since the thermocouples are exposed to many reactive materials, monitoring the ageing is important. This can be monitored by comparing the sample temperature to the furnace or gradient heater temperatures. After a number of measurement runs, the temperature difference will change indicating ageing of the thermocouples. Platinum, for example, is frequently used due to its high inertness to oxygen and many oxides but it reacts readily with Pb, Te, Sb, Si and other elements often found in thermoelectric materials. During a measurement run and sample mounting, poor electrical or thermal contact and other instrument errors can be identified by examining the voltage *vs.* temperature difference curves for hysteresis. For non-reactive samples, the heating and cooling curves of the Seebeck coefficient should be identical, and the same is true for repeated measurement (if the first cooling and second heating curves agree but the rest do not, the sample properties are most likely changing). During sample mounting, 2-point *I–V* curves or resistances between two electrical contacts, including current contacts in combined Seebeck and resistivity systems, can help identify bad electrical contacts.

As with hysteresis, if the Seebeck coefficient depends on the heating rate and size or direction of the temperature difference employed there is likely bad thermal contact between the sample and thermocouples. When measuring in inert gas atmospheres (or air), the Seebeck coefficient should not depend on the gas pressure as this is an indication of bad thermal contact between the sample and thermocouples. This is also visible in Fig. 3a where data below 400 K are measured in air.

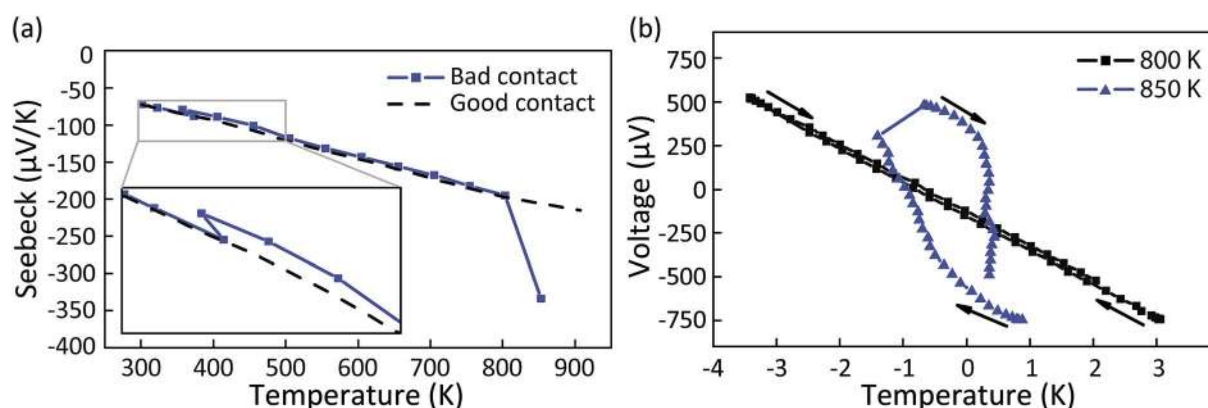

Fig. 3 Example of the effect of bad thermal contact in Seebeck coefficient measurements. (a) A sample was measured from 300 K to 900 K both with good (dashed black line) and bad thermal contact between the sample and thermocouples (solid blue line and square symbols). (b) The raw voltage *vs.* temperature difference plots at 800 K (squares) and 850 K (triangles) for the measurement with bad thermal contact.

Published on 23 September 2014. Downloaded by California Institute of Technology on 20/03/2015 15:15:34.

For the measurement with bad thermal contact a change in the measurement is observed when the chamber is evacuated. In air the two measurements agree since the air improves the thermal contact. This is an early indication of bad thermal contact and the data quality is expected to be bad. In some instruments inert gasses are used to improve thermal contact.

Electrical resistivity

Even though resistivity measurements are often regarded as routine, they are still prone to large errors. The most widely used method is the linear 4-point method with bar-shaped samples as shown in Fig. 4a. Current is passed from one end to the other while the voltage is being measured at two intermediate points. The voltage contacts should be placed sufficiently far from the ends to ensure a uniform current distribution in the bar at and between the voltage contacts (usually placed at 1/3 and 2/3 of the sample length). The resistivity is $\rho = R \times A/l$ where R is the measured 4-point resistance, A is the cross sectional area, and l is the separation of the voltage contacts. The resistivity is therefore highly sensitive to errors in the geometric factor A/l which can easily be in excess of 5%. If the sample is not a parallelepiped, appropriate geometric factors need to be found, either analytically or numerically, *e.g.* from finite element methods. The voltage contacts should be narrow along the length of the sample to avoid uncertainty in l. This can be a problem when resistivity and Seebeck coefficient measurements are combined since the thermocouple tips often have a significant size.

Other techniques exist that may be less sensitive to errors in geometric factors. The most widely used of these in thermoelectrics is the van der Pauw technique, Fig. 4d.[54,55] In this technique, the resistivity is obtained from a flat sample of arbitrary shape but uniform thickness with point contacts along its circumference. Since flat samples can be polished to have a uniform thickness (preferably with a variation of 0.005 mm or less, depending on thickness) that can be measured accurately using a micrometer, the error from the geometric factor may be reduced. In this method, the resistivity can be measured directly from hot pressed samples or slices of Bridgman, Stockbarger, or Czochralski grown ingots. The sample geometry is compatible with measurements of all thermoelectric transport properties, and zT can hence be obtained using only one sample.[18]

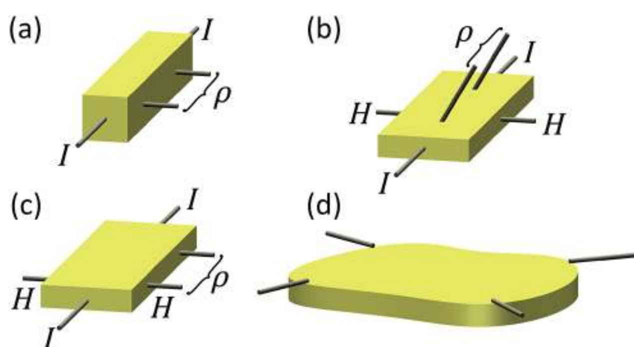

Fig. 4 Four different samples and contact arrangements for resistivity and Hall effect measurements: (a) contact arrangement and optimal sample geometry for only resistivity measurements on bar samples; (b) 6-point and (c) 5-point geometries for combined resistivity and Hall effect measurements with sample geometry optimized for Hall effect measurements; (d) for combined resistivity and Hall effect measurement with the van der Pauw method. In (a)–(c), contacts for the applied current are marked with an I, contacts for resistivity measurements with ρ, and contacts for Hall effect with H. In (d), resistivity measurements are performed by applying current between adjacent contacts while Hall effect measurements are performed with current along a diagonal. This is further discussed in ref. 18.

The variation in electrical resistivity when using the 4-point bar method can be as high as 10% at 500 K,[45] twice that in Seebeck coefficient. The reason for the high scatter is mainly errors in determining the geometric factor,[56–58] indicating that this is indeed important in obtaining accurate resistivities. In the PPMS several options exist for measuring the electrical resistivity. Leads are attached with conducting adhesive, such as silver containing epoxy, which can lead to excessively large contact areas that reduce the accuracy.

Errors can also be caused by inaccurate temperature determination, which can be caused by poor thermal contact between the sample and the mass the thermocouple is attached to. Additionally, the thermocouples can act as cold or hot fingers. The first should be avoided especially in systems that heat the sample with heater blocks in direct contact with the sample. Other systems have a furnace-like heating zone where the sample is radiatively heated. In this case, caution is also needed as high temperature measurements are usually done under vacuum, which means the temperature profile inside the furnace might not be uniform without convection. The commercial ZEM system uses a furnace together with partial back-filled helium so the temperature profile could be quite uniform. However, as long rods are used for the voltage contacts and it is common to apply only a minimum amount of pressure against the sample, this makes temperature reading likely to be either lower or higher than the real sample temperature due to the cold and hot finger effects.

Even a subtle change in measurement procedure can significantly change results. For example Fig. 5 shows the resistivity of n-type PbTe and PbSe that was significantly underestimated (the gray dots) due to an overestimation of the sample temperature. A similar problem may be seen in ref. 14 and 59. A substrate was inserted between the sample and the heater block to protect the sample which resulted in poor thermal contact with the thermocouple.[18] The error is much higher at high temperature where radiative cooling is strongest and the change in resistivity with temperature is high. This error can be detected and avoided two ways: one is by using an insulation shield that reduces the radiation loss from the surface of the sample to the cold chamber wall, shown by blue dots in (a), the other is by directly attaching the thermocouple to the sample, yellow open squares in (a). Designing the system to avoid excessive radiation loss from sample surface is preferable as thermocouple attachment adds complication, possibility of chemical reaction, and user variability. Insulating the sample space using either a radiation shield made of aluminum with ceramic coating (green open triangles in (b)) or 2 mm thick glass

 This journal is © The Royal Society of Chemistry 2015

Published on 23 September 2014. Downloaded by California Institute of Technology on 20/03/2015 15:15:34.

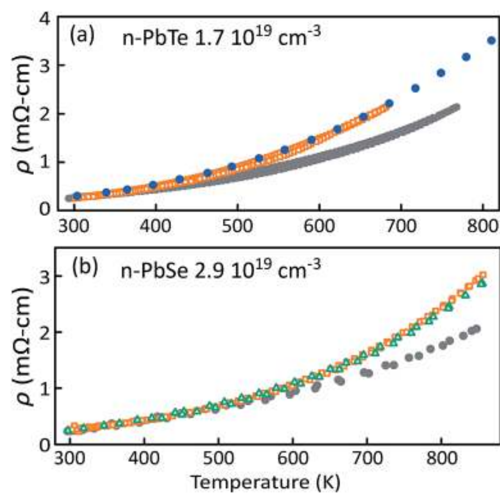

Fig. 5 Resistivity measurement of (a) n type PbTe and (b) n type PbSe using a van der Pauw setup as described in ref. 18. Results shown as grey dots are underestimated due to inaccurate temperature determination as a result of poor thermal contact between sample and heater block. Two effective ways to mitigate this is by either applying insulation/radiation shielding around the sample, shown by blue dots in (a), and yellow open squares and green triangles in (b), or by making direct contact between thermocouple and sample, shown by yellow open squares in (a).

wool (yellow open squares in (b)) makes the sample temperature measurement sufficiently accurate.

There are a number of offsets that have to be accounted for in resistance measurements. There are constant or slowly varying voltage offsets which mainly arise from the Seebeck effect when temperature gradients are present. These may arise both in the sample, leads, and at junctions between dissimilar metals, such as vacuum feedthroughs and other connectors. These are removed by measuring the voltage as a function of applied current instead of simply measuring the voltage under constant applied current.

In all resistivity measurements, a current sufficiently low to avoid significant Joule heating should be used. In thermoelectrics, there is a further complication due to the high Peltier effect.[9] Heat is transported by the current from one contact to the other creating a temperature gradient, which in turn leads to Seebeck voltages.[10] This causes an overestimation of the resistance for both positive and negative Seebeck coefficients.[60,61] To reduce these errors either AC or pulsed DC measurements, where the voltage is measured before and after turning the current on, are used. This also removes constant offset voltages from the Seebeck effect. Carefully heat sinking the sample can further help reduce the errors from the Peltier effect. In DC measurements, switching the current direction can help minimizing the temperature gradient established.

A simple experimental criterion is that repeated raw resistance measurements should not show a systematic change, which is usually caused by the Peltier effect. Changes in resistivity in repeated full measurements are often due to Joule heating of the sample. The quality of the contacts is best tested with 2-point I–V curves: nonlinearity at low voltage indicates poor electrical contact while a curvature at higher currents is most likely caused by the Peltier effect or Joule heating. If I–V sweeps are not possible, 2-point resistance measurements can be used.

If AC measurements are used, the frequency should be chosen sufficiently high to suppress the Peltier effect, usually some tens of hertz. A thermal time constant can be estimated as $\tau = l^2/D_T$, where l is the distance between the voltage contacts and D_T is the thermal diffusivity. The error from the Peltier effect is low for frequencies significantly greater than τ^{-1}. Since the measurement leads have a finite capacitance, low currents and high frequencies lead to current loss in the wires. This current is deposited as charge in the wires and does not contribute to the measured signal, causing a too low resistance. Generally, all circuits can be described as a capacitor and a resistor in parallel. Additionally, to avoid noise in frequency sensitive measurements, the base frequency should be chosen different from the power line frequency and integer multiples or fractions of this.

Charge carrier concentration and mobility

Even though the charge carrier concentration is not necessary for calculating zT, it is still very important since all transport properties depend strongly upon it. It provides an important reference frame for characterizing and identifying the cause of changes in transport properties.

In heavily doped semiconductors such as thermoelectrics, the charge carrier concentration is usually calculated from the Hall coefficient measured on a flat sample in a magnetic field. The Hall voltage V_H is the voltage arising perpendicular to both the field and current direction. The Hall resistance is $R_\perp = V_H/I$ and Hall coefficient $R_H = R_\perp d/B$. d is the sample thickness and B is the perpendicular field strength. Since the current distribution does not have to be uniform, flat and wide samples are usually preferred to samples with square cross sectional area of the same size since these allow the same current and give a high $R_\perp$ due to the low thickness.[62] The traditional 5 and 6-point measurement geometries for combined Hall effect and resistivity measurements are shown in Fig. 4c and b, respectively. A flat sample is less appropriate for resistivity measurements than one with square cross section since the current distribution is less uniform. Combining Hall effect measurements with van der Pauw resistivity reduces this problem and allows a simpler setup with 4 contacts instead of the 5 and 6-point geometries.[18,54,55] In addition, the van der Pauw configuration can be used to avoid the need for switching the magnetic field[63–67] (see below).

Inspired by the free electron model, the Hall carrier concentration is calculated as $n_H = 1/eR_H$ and will be positive for holes and negative for electrons.[62] e is the elementary charge. If the resistivity ρ is also known, the Hall mobility can be calculated as $\mu_H = R_H/\rho$. The Hall carrier concentration is related to the true carrier concentration n by $n = r_H n_H$. r_H is the Hall factor which is generally only equal or close to 1 in the free

Published on 23 September 2014. Downloaded by California Institute of Technology on 20/03/2015 15:15:34.

electron model and the limit of high doping levels in a single parabolic band.[68] In other cases, either appropriate modelling using single or multi band models[15,31,69–72] or *ab initio* calculations are necessary for estimating the true carrier concentration.[73] In complex band structures or for bipolar samples, r_H can deviate strongly from 1. Despite the ambiguity, the Hall carrier concentration is an excellent way to compare relative carrier concentrations within the same materials system (with similar band structure).

The challenges associated with measuring the Hall coefficient are generally the same as for resistivity measurements. In addition, there is also a resistive offset when the voltage contacts are not placed directly across from each other but are displaced slightly along the current path. The Hall signal is usually very low ($R_\perp \approx 63$ μΩ for $n_H = 10^{20}$ cm^{-3}, $B = 1$ T, and $d = 1$ mm) and can be orders of magnitude lower than the voltage offset. For this reason, two magnetic fields (*e.g.*, on/off or with opposite directions) are often used to remove offsets. Especially for metals (or semiconductors with very high doping levels) and intrinsic or bipolar semiconductors the Hall signal can be very low. In intrinsic semiconductors, the resistivity changes rapidly with temperature and hence Joule heating can strongly affect the offset resistance, making Hall effect measurements difficult and noisy.

For high mobility samples there is also an offset from the magneto resistance; however, this does not depend on the field orientation and can be subtracted by reversing the field direction rather than switching it on and off.[18] Alternatively, several points on a $V(B)$ curve including both positive and negative B can be used. In such a curve, magneto resistance would lead to a parabolic curve shape while the Hall effect is primarily linear (always an odd function of the field strength), allowing separation of the two.

An alternative method which is most easily implemented in the van der Pauw configuration is to use the altered reciprocity relations for the measured resistances.[63–65] Without an applied magnetic field, interchanging the voltage and current contacts leads to the same measured resistance (known as reciprocity); however, in an applied magnetic field this is only true if the magnetic field is reversed (known as reverse field reciprocity).[66]

The difference between the two methods is illustrated in Fig. 6. In the field reversal method, the Hall resistance is calculated as $R_\perp = R^{(a)} - R^{(b)}$ where $R^{(a)}$ and $R^{(b)}$ are the resistances measured with the configurations in panel (a) and (b), respectively. Alternatively, using the reverse field reciprocity, the Hall coefficient can be calculated as $R_\perp = R^{(a)} - R^{(c)}$.[65,67] Both methods remove both magneto resistance and resistive offsets. By using the reverse field reciprocity the necessity for inverting the magnetic field is removed. This can both reduce the measurement time and reduce the liquid helium consumption when using cryomagnets such as in a PPMS.

Due to the low signal level, accurate nanovoltmeters and shielded cables are necessary for measuring the Hall coefficient.[18] All measurement leads should be mechanically fixed to reduce errors from wires due to magnetic induction forces. In sensitive measurements, the signal can be overlaid by an induced voltage arising from leads vibrating in the magnetic field. If this coincides with the frequency in AC measurements, this voltage cannot be eliminated by lock-in techniques.

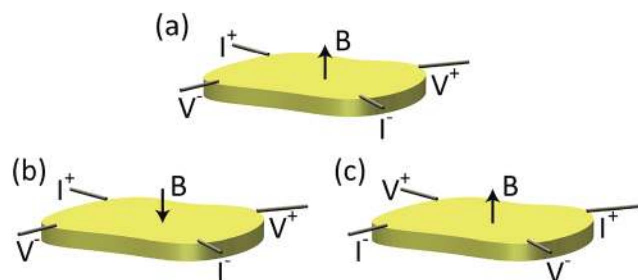

Fig. 6 Three van der Pauw contact designations for illustrating the reverse field reciprocity in Hall effect measurements. The Hall resistance can be calculated from panels (a) and (b) or (a) and (c) as $R_\perp = R^{(a)} - R^{(b)} = R^{(a)} - R^{(c)}$. Due to the reverse field reciprocity $R^{(b)} = R^{(c)}$.

Thermal conductivity

Many methods exist for measuring thermal conductivity, κ. While the most frequently used method today is flash diffusivity,[74–76] (see Fig. 7a) traditionally direct methods were employed (Fig. 7b). Since flash diffusivity also requires measurement of the heat capacity and density these are also covered in this section.

Other methods also exist. One example is the thermal van der Pauw method,[77] which illustrates the fundamental analogy between thermal end electrical conduction. The Harman method[78,79] for directly measuring zT is also frequently used. In

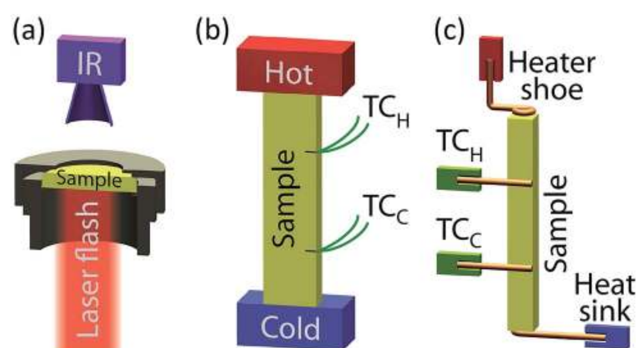

Fig. 7 Geometries for measuring thermal diffusivity with the laser flash method, (a), thermal conductivity with the steady-state method, (b), and in the PPMS TTO, (c). In (a), a short laser pulse is applied to the bottom of a sample (shown in a sample holder) and the resulting temperature rise on the top is monitored with an IR camera. In (b), a constant power is applied to a heater at the top of a sample (red) while the temperature is monitored along its length with thermocouples inserted in small holes (green wires). The thermal conductivity is calculated when steady-state has been reached. In (c), a heat pulse is applied to a heater shoe (red) at the top of a sample while the temperature response is monitored with thermometers (green) along its length and the thermal conductivity is calculated from the transient. This sample and contact arrangement is also used for Seebeck and resistivity measurements. In (b) and (c) the sample is heat sunk at the bottom (blue). Samples are shown in yellow.

This journal is © The Royal Society of Chemistry 2015

Published on 23 September 2014. Downloaded by California Institute of Technology on 20/03/2015 15:15:34.

this method, zT is calculated from the difference in resistance with very low frequency (with Peltier effect) and high frequency (only resistive part). Both methods fundamentally have the same difficulties as direct thermal conductivity measurements and are hence not discussed individually.

While most of the techniques for measuring resistivity and Seebeck coefficient also work for thin films, thermal conductivity needs to be measured with specialized techniques. The most widely used of these are the 3ω [80,81] and time domain thermoreflectance (TDTR) techniques.[82–84]

Direct measurements

Before the development of the flash diffusivity method,[76] methods directly using the Fourier equation, $q = -\kappa A\nabla T$, were most common. Here q is the heat flow along the sample, A is the cross sectional area, and ∇T is the temperature gradient. The heat flow needs to be corrected for loss through heater and thermometer wires and radiation. While this works well at low temperatures (below approximately 200 K), the difficulty in accurately correcting for radiation loss limits the accuracy at higher temperatures.[85] In these methods the sample needs to be in good thermal contact with the heater, heat sink, and thermocouples while being thermally insulated from the surroundings. For small temperature differences between the sample and surroundings, the heat loss due to radiation is $q_{\text{rad}} = \varepsilon A\Delta T T^3$, where ε is the emissivity, A is the surface area, T is the temperature, and ΔT the temperature difference between sample and surroundings.[20] Hence, accurate radiation correction becomes much more important at high temperatures.

A steady-state setup described by Zaitsev *et al.*[86] uses a radiation shield thermally anchored to both the heater and heat sink to establish a temperature gradient similar to the gradient in the sample. The space between sample and heat shield is filled with thermally insulating powder (alumina or silicate based ceramics) to further reduce the radiation loss, whereas heat loss due to conduction through the powder was calibrated.

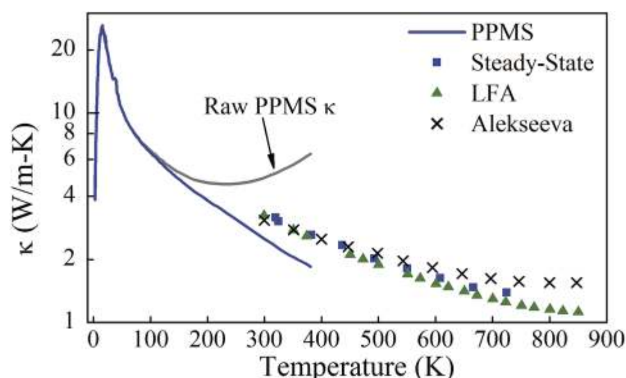

Fig. 8 Comparison of thermal conductivity between the PPMS (blue line), laser flash method (green triangles), Ioffe Institute steady-state method (blue squares) and published data from ref. 87 (black crosses). The same PbSe sample with $n_H = 2.0 \times 10^{19}$ cm^{-3} are used for all measurements except the crosses. The grey line marked as "Raw PPMS κ" is the measured thermal conductivity before correction for radiation loss.

Alekseeva *et al.*[87] reported thermal conductivity of n-type PbSe using this setup and the result is consistent with the laser flash method around room temperature. However, it is noticeably higher at high temperatures, as seen in Fig. 8. This was known at the time and resulted from an underestimated heat loss correction due to the lack of appropriate reference materials. Comparing the steady-state setup with improved heat loss correction to the laser flash method, the results are fairly consistent up to 700 K for n-type PbSe, suggesting the steady-state method as implemented by the Ioffe Institute could be as accurate in this temperature range. This will be thoroughly described in a future publication which will also include a more detailed comparison to results from flash diffusivity. Fig. 8 shows a comparison of results from the same PbSe sample including low temperature data obtained from a PPMS, together with Alekseeva's result from a sample with very similar electrical properties.

In the PPMS the thermal conductivity is measured by a direct transient method where the increase and decrease in temperature between two thermometers is modeled when a square wave heat pulse is applied. The geometry is shown in Fig. 7c. The heat loss through the electrical wires is accounted for through the calibration, while the radiation loss is calculated from the sample surface area and emissivity and is subtracted from the measured thermal conductivity. The latter is difficult since the emissivity is usually not known and the surface area is difficult to calculate since leads are attached with thermally conductive adhesive to the surface of the sample, as shown in Fig. 7c (without the adhesive). This difficulty is clearly visible from Fig. 8, where the radiation loss is clearly overestimated. The radiation correction is visible from about 100 K and becomes a significant fraction of the thermal conductivity at approximately 200 K. The emissivity was set to 1 (an overestimate) while the sample surface area without attached leads was used (an underestimate). These errors oppose each other and the resulting correction in this case is an overestimate resulting in an underestimated thermal conductivity. A more comprehensive comparison between the PPMS and LFA can be found in ref. 88, including a thorough discussion of the radiation correction and problems with choosing an appropriate emissivity.

Flash diffusivity

In the flash diffusivity method, the thermal conductivity is calculated as $\kappa = D_T d C_p$ where D_T is thermal diffusivity, d is density, and C_p is the constant pressure heat capacity. In this method, a short heat pulse (often by laser flash) is applied to one side of a thin sample, while the temperature of the other side is monitored continuously. The temperature will rise to a maximum, after which it will decay. In the original method, which makes an excellent check for the data, the time for the temperature to increase to half-maximum, $T_{1/2}$, is used to calculated the thermal diffusivity $D_T = 1.38d^2/\pi T_{1/2}$ where d is the thickness.[76] This is derived assuming only axial flow of heat and no heat loss, and hence the sample thickness should be much smaller than the diameter and $T_{1/2}$ should be kept in the

Published on 23 September 2014. Downloaded by California Institute of Technology on 20/03/2015 15:15:34.

range from a millisecond to no more than a few seconds, but always much larger than the pulse duration.

A correction was proposed by Cowan[89] to account for heat losses on the sample faces, still assuming axial flow. He used the temperature at $T_{1/2}$ and 5 or 10 times $T_{1/2}$ to also estimate the heat loss terms occurring in his revised expression for α. Alternatively, Clark and Taylor[90] proposed a method only using the heating section of the transient. This method also accounts for heat loss at the sides of the sample and finite heat pulse duration. These two methods are usually recommended[24] but another method by Cape and Lehman[91] is also frequently used. In the modern implementation of these methods, the expressions are fitted to the entire transient to obtain better estimates of the heat loss terms and corrections for the pulse width and shape can also be applied.

In the comparison to the steady-state method and PPMS data in Fig. 8, the laser flash data is believed to be more accurate since it is less susceptible to errors from radiation loss corrections. However, the Ioffe Institute steady-state method does seem to produce good results below 700 K (the highest reported temperature) and may provide a useful method for measuring thermal conductivity, especially when the heat capacity is not easily obtained, such as across phase transitions *etc.*[92,93]

The scatter in thermal diffusivity between different laboratories can be as high as 5% at room temperature and almost 10% at 500 K.[24] Much of this can be ascribed to variations in measured thickness. This indicates that a constant and accurately measured thickness is as important for diffusivity measurements as the geometric factor is for resistivity measurements. Another possible source of error is the graphite coating often employed in diffusivity measurements. While this ensures a high emissivity and hence good absorption of the laser pulse and maximum detector signal, too thick coatings or poor adhesion to the sample can cause significant errors, especially for thin samples.

Heat capacity

When using flash diffusivity, measurement of the heat capacity is also necessary to obtain thermal conductivity. While some commercial flash diffusivity systems can estimate the heat capacity relative to a standard, this is often inaccurate and can lead to underestimates of thermal conductivity. Instead, drop calorimetry provides the best accuracy (especially at high temperatures) but today differential scanning calorimetry (DSC) is more frequently used. As an example, Toberer *et al.*[25] measured a room temperature C_p on $Ba_8Ga_{16}Ge_{30}$ of 0.23 J g^{-1} K^{-1} using a laser flash analysis (LFA) setup. This was later corrected by the same group to 0.30 J g^{-1} K^{-1} using DSC, much closer to the Dulong–Petit value of 0.307 J g^{-1} K^{-1} (see below).[31] In a DSC, the heat capacity is measured relative to a standard, usually sapphire. First a baseline is measured with empty sample holders, then the sample and reference is measured. Often, the baseline is measured again after measuring the sample to check for changes in baseline during the measurement.[24] The reference should be chosen to give a signal close to the measured sample to reduce errors. In the PPMS heat capacity option the heat capacity is measured without a reference. First a baseline is measured with only thermal grease in the sample holder, then the sample is added and measured. The heat capacity is calculated from the heating and cooling transient when applying a heat pulse using the two-tau method.[94]

A scatter in heat capacity of 15% has been observed.[24] The primary sources of error are operator error or inexperience, baseline shift and inappropriate reference sample. Heat capacity is the measurement most sensitive to operator error and inexperience.[24] Above the Debye temperature and in the absence of phase transitions, C_p normally increases slightly with temperature. The best data quality check is comparison to the Dulong–Petit law which states that the constant volume heat capacity above the Debye temperature is approximately $3k_B$ per atom, or $C_V^{DP} = 3N_Ak_B/M$. C_V^{DP} is the Dulong–Petit heat capacity, k_B the Boltzmann constant, N_A Avogadro's number, and M is the molar mass. C_V is related to C_p by $C_p = C_V^{DP} + 9\alpha^2T/\beta_TD$. α is linear coefficient of thermal expansion, β_T isothermal compressibility, and D density. The measured C_p above the Debye temperature should be close to or slightly higher than the Dulong–Petit value and increase slowly with temperature. When the correction is applied, the measured and calculated heat capacities usually agree within 2%. When the values disagree more than about 5%, extra verification is recommended before using the measured values. If no DSC is available or measured values are unexplainable, the authors recommend using the corrected Dulong–Petit value.

In the example with $Ba_8Ga_{16}Ge_{30}$, both LFA and DSC resulted in a heat capacity that was increasing linearly with temperature. However, the C_p estimated from LFA was lower than the C_V^{DP} = 0.307 J g^{-1} K^{-1} for all temperatures while the DSC values crossed C_V^{DP} slightly above the Debye temperature of approximately 300 K as expected. This is a clear indication that the LFA estimate was unreliable, which the authors also commented upon.

Density and thermal expansion

The last property necessary for calculating thermal conductivity is the density. The geometric density is measured by calculating the volume from the geometry and dimensions of the sample which works well for regularly shaped samples. Density measured using Archimedes' principle (by immersion in a liquid) can overestimate the density relevant for $\kappa = D_TdC_p$ if the liquid is absorbed in the pores. This can be checked by measuring the weight in air both before and after the measurement in the liquid. These measurements are fairly accurate at room temperature and the density is usually assumed to be independent of temperature.[24]

The density as well as resistivity, diffusivity, and thermal conductivity are dependent on the sample dimensions and hence thermal expansion. An analysis by Toberer *et al.*[25] shows that while each property is affected by thermal expansion, both $\rho\kappa$, Seebeck and zT are unaffected by this. This was derived assuming a temperature independent coefficient of linear thermal expansion; however, it can be extended to any temperature dependence of thermal expansion. If the sample

This journal is © The Royal Society of Chemistry 2015

Published on 23 September 2014. Downloaded by California Institute of Technology on 20/03/2015 15:15:34.

has anisotropic thermal expansion and all properties are not measured along the same direction, this is no longer true.

Some commercial LFA software has the capability to correct for thermal expansion. While this can increase the accuracy of the thermal diffusivity and conductivity, it can decrease the accuracy of zT unless the same expansion correction is applied to all the properties affected by thermal expansion (density, resistivity and thermal diffusivity). Since the software from different companies applies this differently, it is important to understand how this is done to avoid introducing errors from the correction.

Conclusion

We have described the most common methods and issues related to measurement of thermoelectric properties of bulk samples. Due to the vast number of different methods employed for measuring the individual properties, no strict guidelines have been given for conducting measurements. Instead, different effects leading to errors have been discussed and signatures of erroneous data and remediation methods have been reviewed. It is hoped that this will aid new researchers as well as young students in the field of thermoelectrics to better understand and appreciate the challenge of conducting high quality measurements.

Even for routinely conducted measurements by experienced groups, differences in zT can be 20% as found by Hsin Wang *et al.*,[24] and uncertainty increases with temperature. The heat capacity is the largest contribution to the error in thermal conductivity which can be significantly reduced by comparison to the Dulong–Petit value. In addition systematic differences due to different techniques in measuring Seebeck coefficient can add on the order of 5% uncertainty, which also increases strongly with temperature. As methodologies change and evolve in the future as they have in the past, this issue will need to be critically revisited.

Acknowledgements

The authors are thankful to Stephen Kang, Hsin Wang, Terry Tritt, Atsushi Yamamoto, and Joshua Martin for measurements, advice and sharing personal experiences. The work was supported by the Danish National Research Foundation (Center for Materials Crystallography, DNRF93). J. de Boor acknowledges endorsement by the Helmholtz Association.

Notes and references

1 G. J. Snyder and E. S. Toberer, *Nat. Mater.*, 2008, **7**, 105–114.
2 L. E. Bell, *Science*, 2008, **321**, 1457–1461.
3 F. J. DiSalvo, *Science*, 1999, **285**, 703–706.
4 A. D. LaLonde, Y. Pei, H. Wang and G. Jeffrey Snyder, *Mater. Today*, 2011, **14**, 526–532.
5 J. H. Yang and T. Caillat, *MRS Bull.*, 2006, **31**, 224–229.
6 D. Samson, M. Kluge, T. Becker and U. Schmid, *Sens. Actuators, A*, 2011, **172**, 240–244.
7 A. Dewan, S. U. Ay, M. N. Karim and H. Beyenal, *J. Power Sources*, 2014, **245**, 129–143.
8 C. B. Vining, *Nat. Mater.*, 2009, **8**, 83–85.
9 D. M. Rowe, *Thermoelectrics Handbook: Macro to Nano*, CRC press, 2006.
10 D. M. Rowe, *CRC handbook of thermoelectrics*, CRC press, 2010.
11 T. C. Harman, D. L. Spears and M. P. Walsh, *J. Electron. Mater.*, 1999, **28**, L1–L5.
12 T. C. Harman, P. J. Taylor, D. L. Spears and M. P. Walsh, *J. Electron. Mater.*, 2000, **29**, L1–L2.
13 C. J. Vineis, T. C. Harman, S. D. Calawa, M. P. Walsh, R. E. Reeder, R. Singh and A. Shakouri, *Phys. Rev. B: Condens. Matter Mater. Phys.*, 2008, **77**, 235202.
14 H. Wang, Y. Pei, A. D. LaLonde and G. J. Snyder, *Adv. Mater.*, 2011, **23**, 1366–1370.
15 H. Wang, Y. Pei, A. D. LaLonde and G. J. Snyder, *Proc. Natl. Acad. Sci. U. S. A.*, 2012, **109**, 9705–9709.
16 J. Martin, *Rev. Sci. Instrum.*, 2012, **83**, 065101–065109.
17 J. Martin, *Meas. Sci. Technol.*, 2013, **24**, 085601.
18 K. A. Borup, E. S. Toberer, L. D. Zoltan, G. Nakatsukasa, M. Errico, J.-P. Fleurial, B. B. Iversen and G. J. Snyder, *Rev. Sci. Instrum.*, 2012, **83**, 123902.
19 S. Iwanaga, E. S. Toberer, A. LaLonde and G. J. Snyder, *Rev. Sci. Instrum.*, 2011, **82**, 063905.
20 T. M. Tritt, *Thermal conductivity: theory, properties, and applications*, Springer, 2004.
21 R. P. Tye, *Thermal conductivity*, Academic Press London, 1969.
22 J. Parrott and A. Stuckes, *Thermal Conductivity of Solids*, 1975.
23 E. S. Toberer, L. L. Baranowski and C. Dames, *Annu. Rev. Mater. Sci.*, 2012, **42**, 179–209.
24 H. Wang, W. Porter, H. Böttner, J. König, L. Chen, S. Bai, T. Tritt, A. Mayolet, J. Senawiratne, C. Smith, F. Harris, P. Gilbert, J. Sharp, J. Lo, H. Kleinke and L. Kiss, *J. Electron. Mater.*, 2013, **42**, 1073–1084.
25 E. S. Toberer, M. Christensen, B. B. Iversen and G. J. Snyder, *Phys. Rev. B: Condens. Matter Mater. Phys.*, 2008, **77**, 075203.
26 J. He, J. Androulakis, M. G. Kanatzidis and V. P. Dravid, *Nano Lett.*, 2012, **12**, 343–347.
27 M. Ohta, K. Biswas, S. H. Lo, J. He, D. Y. Chung, V. P. Dravid and M. G. Kanatzidis, *Adv. Energy Mater.*, 2012, **2**, 1117–1123.
28 S. M. Kauzlarich, *Chemistry, structure, and bonding of Zintl phases and ions*, VCH New York, 1996.
29 S. C. Sevov, in *Intermetallic Compounds - Principles and Practice*, John Wiley & Sons, Ltd, 2002, pp. 113–132.
30 S. M. Kauzlarich, S. R. Brown and G. Jeffrey Snyder, *Dalton Trans.*, 2007, 2099–2107.
31 A. F. May, E. S. Toberer, A. Saramat and G. J. Snyder, *Phys. Rev. B: Condens. Matter Mater. Phys.*, 2009, **80**, 125205.
32 E. S. Toberer, A. F. May and G. J. Snyder, *Chem. Mater.*, 2009, **22**, 624–634.
33 M. Søndergaard, M. Christensen, K. A. Borup, H. Yin and B. B. Iversen, *Acta Mater.*, 2012, **60**, 5745–5751.
34 M. Søndergaard, M. Christensen, K. Borup, H. Yin and B. Iversen, *J. Mater. Sci.*, 2013, **48**, 2002–2008.

View Article Online

Published on 23 September 2014. Downloaded by California Institute of Technology on 20/03/2015 15:15:34.

35 H. Yin, M. Christensen, N. Lock and B. B. Iversen, *Appl. Phys. Lett.*, 2012, **101**, 043901.
36 T. Dasgupta, C. Stiewe, A. Sesselmann, H. Yin, B. Iversen and E. Mueller, *J. Appl. Phys.*, 2013, **113**, 103708.
37 M. Beekman, M. Baitinger, H. Borrmann, W. Schnelle, K. Meier, G. S. Nolas and Y. Grin, *J. Am. Chem. Soc.*, 2009, **131**, 9642–9643.
38 N. Chen, F. Gascoin, G. J. Snyder, E. Müller, G. Karpinski and C. Stiewe, *Appl. Phys. Lett.*, 2005, **87**, 171903.
39 D. Platzek, G. Karpinski, C. Stiewe, P. Ziolkowski, C. Drasar and E. Muller, *Potential-Seebeck-microprobe (PSM): measuring the spatial resolution of the Seebeck coefficient and the electric potential*, Clemson, South Carolina, USA, 2005.
40 H. L. Ni, X. B. Zhao, G. Karpinski and E. Müller, *J. Mater. Sci.*, 2005, **40**, 605–608.
41 S. Iwanaga and G. J. Snyder, *J. Electron. Mater.*, 2012, **41**, 1667–1674.
42 A. F. May, J.-P. Fleurial and G. J. Snyder, *Phys. Rev. B: Condens. Matter Mater. Phys.*, 2008, **78**, 125205.
43 M. Sondergaard, M. Christensen, L. Bjerg, K. A. Borup, P. Sun, F. Steglich and B. B. Iversen, *Dalton Trans.*, 2012, **41**, 1278–1283.
44 M. Christensen, S. Johnsen, M. Søndergaard, J. Overgaard, H. Birkedal and B. B. Iversen, *Chem. Mater.*, 2008, **21**, 122–127.
45 H. Wang, W. Porter, H. Böttner, J. König, L. Chen, S. Bai, T. Tritt, A. Mayolet, J. Senawiratne, C. Smith, F. Harris, P. Gilbert, J. Sharp, J. Lo, H. Kleinke and L. Kiss, *J. Electron. Mater.*, 2013, **42**, 654–664.
46 N. D. Lowhorn, W. Wong-Ng, W. Zhang, Z. Q. Lu, M. Otani, E. Thomas, M. Green, T. N. Tran, N. Dilley, S. Ghamaty, N. Elsner, T. Hogan, A. D. Downey, Q. Jie, Q. Li, H. Obara, J. Sharp, C. Caylor, R. Venkatasubramanian, R. Willigan, J. Yang, J. Martin, G. Nolas, B. Edwards and T. Tritt, *Appl. Phys. A: Mater. Sci. Process.*, 2009, **94**, 231–234.
47 Z. Lu, N. D. Lowhorn, W. Wong-Ng, W. Zhang, M. Otani, E. E. Thomas, M. L. Green and T. N. Tran, *J. Res. Natl. Inst. Stand. Technol.*, 2009, **114**, 37–55.
48 J. Martin, T. Tritt and C. Uher, *J. Appl. Phys.*, 2010, **108**, 121101.
49 J. de Boor and E. Muller, *Rev. Sci. Instrum.*, 2013, **84**, 065102.
50 P. H. M. Bottger, E. Flage-Larsen, O. B. Karlsen and T. G. Finstad, *Rev. Sci. Instrum.*, 2012, **83**, 025101.
51 R. L. Kallaher, C. A. Latham and F. Sharifi, *Rev. Sci. Instrum.*, 2013, **84**, 013907.
52 C. Wood, D. Zoltan and G. Stapfer, *Rev. Sci. Instrum.*, 1985, **56**, 719–722.
53 A. Guan, H. Wang, H. Jin, W. Chu, Y. Guo and G. Lu, *Rev. Sci. Instrum.*, 2013, **84**, 043903.
54 L. J. van der Pauw, *Philips Res. Rep.*, 1958, **13**, 1.
55 L. J. van der Pauw, *Philips Tech. Rev.*, 1958, **20**, 220.
56 A. T. Burkov, A. Heinrich, P. P. Konstantinov, T. Nakama and K. Yagasaki, *Meas. Sci. Technol.*, 2001, **12**, 264.
57 V. Ponnambalam, S. Lindsey, N. S. Hickman and T. M. Tritt, *Rev. Sci. Instrum.*, 2006, **77**, 073904.
58 B. Céline, B. David and D. Nita, *Meas. Sci. Technol.*, 2012, **23**, 035603.
59 A. D. LaLonde, Y. Pei and G. J. Snyder, *Energy Environ. Sci.*, 2011, **4**, 2090–2096.
60 C. G. M. Kirby and M. J. Laubitz, *Metrologia*, 1973, **9**, 103.
61 M. V. Cheremisin, *Peltier effect induced correction to ohmic resistance*, Washington, DC, USA, 2001.
62 E. H. Putley, *The Hall effect and related phenomena*, Butterworths, London, 1960.
63 R. Spal, *J. Appl. Phys.*, 1980, **51**, 4221–4225.
64 M. Büttiker, *Phys. Rev. Lett.*, 1986, **57**, 1761–1764.
65 H. H. Sample, W. J. Bruno, S. B. Sample and E. K. Sichel, *J. Appl. Phys.*, 1987, **61**, 1079–1084.
66 L. L. Soethout, H. v. Kempen, J. T. P. W. v. Maarseveen, P. A. Schroeder and P. Wyder, *J. Phys. F: Met. Phys.*, 1987, **17**, L129.
67 M. Levy and M. P. Sarachik, *Rev. Sci. Instrum.*, 1989, **60**, 1342–1343.
68 V. I. Fistul, *Heavily doped semiconductors*, Plenum Press, New York, 1969.
69 Y. Z. Pei, X. Y. Shi, A. LaLonde, H. Wang, L. D. Chen and G. J. Snyder, *Nature*, 2011, **473**, 66–69.
70 L.-D. Zhao, J. He, S. Hao, C.-I. Wu, T. P. Hogan, C. Wolverton, V. P. Dravid and M. G. Kanatzidis, *J. Am. Chem. Soc.*, 2012, **134**, 16327–16336.
71 H. Wang, A. D. LaLonde, Y. Pei and G. J. Snyder, *Adv. Funct. Mater.*, 2013, **23**, 1586–1596.
72 X. Liu, T. Zhu, H. Wang, L. Hu, H. Xie, G. Jiang, G. J. Snyder and X. Zhao, *Adv. Energy Mater.*, 2013, **3**, 1238–1244.
73 N. W. Ashcroft and N. D. Mermin, *Solid state physics*, CBS Publishing, Philadelphia, 1988.
74 J. W. Vandersande, A. Zoltan and C. Wood, *Int. J. Thermophys.*, 1989, **10**, 251–257.
75 C. B. Vining, A. Zoltan and J. W. Vandersande, *Int. J. Thermophys.*, 1989, **10**, 259–268.
76 W. J. Parker, R. J. Jenkins, C. P. Butler and G. L. Abbott, *J. Appl. Phys.*, 1961, **32**, 1679–1684.
77 J. de Boor and V. Schmidt, *Adv. Mater.*, 2010, **22**, 4303–4307.
78 T. C. Harman, J. H. Cahn and M. J. Logan, *J. Appl. Phys.*, 1959, **30**, 1351–1359.
79 X. Y. Ao, J. de Boor and V. Schmidt, *Adv. Energy Mater.*, 2011, **1**, 1007–1011.
80 D. G. Cahill and R. O. Pohl, *Phys. Rev. B: Condens. Matter Mater. Phys.*, 1987, **35**, 4067–4073.
81 T. Tong and A. Majumdar, *Rev. Sci. Instrum.*, 2006, **77**, 104902.
82 C. A. Paddock and G. L. Eesley, *J. Appl. Phys.*, 1986, **60**, 285–290.
83 D. G. Cahill, *Rev. Sci. Instrum.*, 2004, **75**, 5119–5122.
84 Y. K. Koh, S. L. Singer, W. Kim, J. M. O. Zide, H. Lu, D. G. Cahill, A. Majumdar and A. C. Gossard, *J. Appl. Phys.*, 2009, **105**, 054303.
85 A. L. Pope, B. Zawilski and T. M. Tritt, *Cryogenics*, 2001, **41**, 725–731.
86 V. K. Zaitsev, M. I. Fedorov, E. A. Gurieva, I. S. Eremin, P. P. Konstantinov, A. Y. Samunin and M. V. Vedernikov, *Phys. Rev. B: Condens. Matter Mater. Phys.*, 2006, **74**, 045207.

This journal is © The Royal Society of Chemistry 2015

87 G. T. Alekseeva, E. A. Gurieva, P. P. Konstantinov, L. V. Prokofeva and M. I. Fedorov, *Semiconductors*, 1996, **30**, 1125–1127.
88 E. Müller, C. Stiewe, D. Rowe and S. Williams, in *Thermoelectrics Handbook: Macro to nano*, ed. D. M. Rowe, 2005, p. 26.
89 R. D. Cowan, *J. Appl. Phys.*, 1963, **34**, 926–927.
90 L. M. Clark III and R. E. Taylor, *J. Appl. Phys.*, 1975, **46**, 714–719.
91 J. A. Cape and G. W. Lehman, *J. Appl. Phys.*, 1963, **34**, 1909–1913.
92 D. R. Brown, T. Day, K. A. Borup, S. Christensen, B. B. Iversen and G. J. Snyder, *APL Mater.*, 2013, **1**, 52107.
93 H. Liu, X. Yuan, P. Lu, X. Shi, F. Xu, Y. He, Y. Tang, S. Bai, W. Zhang, L. Chen, Y. Lin, L. Shi, H. Lin, X. Gao, X. Zhang, H. Chi and C. Uher, *Adv. Mater.*, 2013, **25**, 6607–6612.
94 J. S. Hwang, K. J. Lin and C. Tien, *Rev. Sci. Instrum.*, 1997, **68**, 94–101.

Published on 23 September 2014. Downloaded by California Institute of Technology on 20/03/2015 15:15:34.